Propagation in a Dielectric-Loaded Parallel Plane Waveguide*

MARVIN COHN†

Summary—A theoretical analysis of wave propagation in a parallel plane waveguide partially filled with a dielectric is performed. This transmission line is a symmetrical three-region structure consisting of two infinite parallel conducting planes with a dielectric slab of rectangular cross section between and contacting each of the planes. It has been found that TEM and TM modes cannot propagate on this structure. This investigation is concerned with TE modes, although hybrid modes can also propagate on this line. The lowest order TE mode, which is the dominant mode, has no cutoff and hence is inherently suited to extremely wide bandwidth operation. Equations have been presented for the field components, guide wavelength, cutoff criteria, power handling capabilities, wall losses, and dielectric losses as a function of the operating wavelength, waveguide dimensions, and material constants. In the case of the dominant mode, design curves covering a large range of wavelengths, dimensions, and dielectric constants are presented. For a loosely bound wave, the losses are comparable or less than those of conventional rectangular waveguide and the power handling capacity is an order of magnitude greater.

Introduction

THE structure to be analyzed consists of two infinite parallel conducting planes with a dielectric slab of rectangular cross section between, and contacting each of the planes (see Fig. 1). It will be shown that this line is capable of extremely broad-band and high-power operation and that its losses are comparable to that of conventional rectangular waveguide. It has the disadvantages of being a partially open structure and being larger than conventional guide. In the millimeter wavelength region the last property may, however, be an advantage.

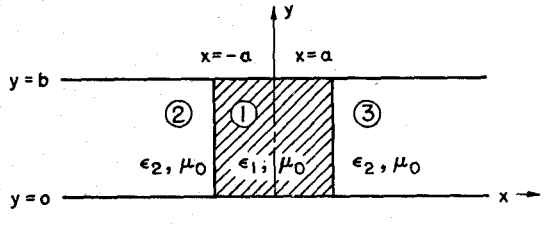

Fig. 1—Cross section of the parallel plane waveguide partially filled with a dielectric. The positive z-direction is out of the paper.

The propagation of TE modes on this line has been theoretically investigated. Expressions are presented for the field intensities, guide wavelength, cutoff conditions, power handling capabilities, wall losses, and dielectric losses as a function of the operating wavelength, waveguide dimensions, and material constants. In the case of the lowest order TE mode, which is the dominant mode of this line, many of these quantities have been computed and plotted to serve as design curves.

It can be shown that both TEM and TM waves cannot be propagated on this line. The propagation of hybrid modes on this type of line has been analyzed by Tischer,[1,2] and in an independent investigation, Moore and Beam[3] have studied both TE and hybrid modes. The report of the latter authors, however, has not been referenced by the principal indexes in the field. The latter paper contains errors in the equations concerning dielectric and metallic losses and in the curve of metallic attenuation. One of the curves showing the cutoff condition for the hybrid modes is also in error.[4]

In a recent paper, Vartanian, Ayres, and Helgesson[5] have shown that improved bandwidth and power handling capabilities can be obtained with a related structure consisting of a dielectric slab centered in a rectangular waveguide.

Interest has been aroused in both this structure and a coaxial line partially filled with a dielectric, which is similar to a parallel plane line wrapped in a circle, because they have properties suitable for use in a nonreciprocal ferrite device.[6–8]

Field Components of the TE Modes

Since the derivation of the field components is available in the paper by Moore and Beam,[3] it will not be repeated here. A report[9] has been published which gives a detailed derivation of the TE mode field components and includes an extensive discussion of the next higher order TE mode.

* Manuscript received by the PGMTT, June 23, 1958; revised manuscript received, December 29, 1958.

† Radiation Lab. The Johns Hopkins University, Baltimore, Md.

[1] F. J. Tischer, "Microwellenleitung mit geringen Verlusten," (Waveguides with small losses), *Arch. elekt. Übertragung*, vol. 7, pp. 592–596; December, 1953.

[2] F. J. Tischer, "The H-guide, a waveguide for microwaves," 1956 IRE Convention Record, pt. 5, pp. 44–47.

[3] R. A. Moore and R. E. Beam, "A duo-dielectric parallel plane waveguide," *Proc. NEC*, vol. 12, pp. 689–705; April, 1957.

[4] During recent communications with R. A. Moore, he has verified the existence of the cited errors.

[5] P. H. Vartanian, W. P. Ayres, and A. L. Helgesson, "Propagation in dielectric slab-loaded rectangular waveguide," IRE Trans. on Microwave Theory and Techniques, Vol. MTT-6, pp. 215–222; April, 1958.

[6] B. J. Duncan, L. Swern, and K. Tomiyasu, "Microwave magnetic field in dielectric-loaded coaxial line," Proc. IRE, vol. 46, pp. 500–502; February, 1958. This qualitative analysis, however, yields an erroneous picture of the field configuration in dielectric-loaded parallel plane line.

[7] M. Cohn, "Parallel plane waveguide partially filled with a dielectric," Proc. IRE, vol. 46, pp. 1952–1953; December, 1958.

[8] K. J. Button, "Theory of non-reciprocal ferrite phase shifters in dielectric-loaded coaxial line," *J. Appl. Phys.*, vol. 29, pp. 998–1000; June, 1958.

[9] M. Cohn, "Parallel Plane Waveguide Partially Filled with a Dielectric," The Johns Hopkins Univ., Radiation Lab., Baltimore, Md., Tech. Rep. No. AF-56; November, 1958.

A cross section of the transmission line to be analyzed and the coordinate system used are shown in Fig. 1. The symmetry of the transmission line causes all solutions to fall into two groups, even and odd modes. These modes are defined by

$$E_{ye}(x) = E_{ye}(-x) \quad \text{and} \quad E_{yo}(x) = -E_{yo}(-x), \quad (1)$$

where the subscripts e and o refer to the even and odd modes, respectively. The expressions for the field components of the even and odd order TE modes in each of the three regions are listed below. The factor $e^{j(\omega t-\beta z)}$, which is common to each of these expressions, has been eliminated in the interest of brevity.

Region 1, even modes

$$H_{x1e} = A_e \frac{\beta}{k_{1e}} \cos k_{1e}x \quad (2a)$$

$$H_{z1e} = jA_e \sin k_{1e}x \quad (2b)$$

$$E_{y1e} = -A_e \frac{\omega\mu_0}{k_{1e}} \cos k_{1e}x \quad (2c)$$

Region 2, even modes

$$H_{x2e} = A_e \frac{\beta}{k_{2e}} (\sin k_{1e}a)e^{k_{2e}(a+x)} \quad (3a)$$

$$H_{z2e} = -jA_e(\sin k_{1e}a)e^{k_{2e}(a+x)} \quad (3b)$$

$$E_{y2e} = -A_e \frac{\omega\mu_0}{k_{2e}} (\sin k_{1e}a)e^{k_{2e}(a+x)} \quad (3c)$$

Region 3, even modes

$$H_{x3e} = A_e \frac{\beta}{k_{2e}} (\sin k_{1e}a)e^{k_{2e}(a-x)} \quad (4a)$$

$$H_{z3e} = jA_e(\sin k_{1e}a)e^{k_{2e}(a-x)} \quad (4b)$$

$$E_{y3e} = -A_e \frac{\omega\mu_0}{k_{2e}} (\sin k_{1e}a)e^{k_{2e}(a-x)} \quad (4c)$$

Region 1, odd modes

$$H_{x1o} = jA_o \frac{\beta}{k_{1o}} \sin k_{1o}x \quad (5a)$$

$$H_{z1o} = A_0 \cos k_{1o}x \quad (5b)$$

$$E_{y1o} = -jA_o \frac{\omega\mu_o}{k_{1o}} \sin k_{1o}x \quad (5c)$$

Region 2, odd modes

$$H_{x2o} = jA_o \frac{\beta}{k_{2o}} (\cos k_{1o}a)e^{k_{2o}(a+x)} \quad (6a)$$

$$H_{z2o} = A_0(\cos k_{1o}a)e^{k_{2o}(a+x)} \quad (6b)$$

$$E_{y2o} = -jA_o \frac{\omega\mu_o}{k_{2o}} (\cos k_{1o}a)e^{k_{2o}(a+x)} \quad (6c)$$

Region 3, odd modes

$$H_{x3o} = -jA_o \frac{\beta}{k_{2o}} (\cos k_{1o}a)e^{k_{2o}(a-x)} \quad (7a)$$

$$H_{z3o} = A_0(\cos k_{1o}a)e^{k_{2o}(a-x)} \quad (7b)$$

$$E_{y3o} = jA_o \frac{\omega\mu_0}{k_{2o}} (\cos k_{1o}a)e^{k_{2o}(a-x)} \quad (7c)$$

A_e and A_o are arbitrary constants.

The inner and outer transverse distribution constants (k_1 and k_2) are related to the propagation constant (β), frequency (ω), and properties of the medium (μ and ϵ) by the following equations:

$$\beta^2 = -k_1^2 + \omega^2\mu_0\epsilon_1 \quad (8)$$

$$\beta^2 = k_2^2 + \omega^2\mu_0\epsilon_2. \quad (9)$$

In order to match boundary conditions at the air-dielectric interfaces ($x = \pm a$), the following conditional equations must be satisfied.

$$k_{2e} = k_{1e} \tan k_{1e}a \quad (10)$$

where $(k_{1e}a)$ must be between o and $\pi/2$, π and $3\pi/2$, etc.

$$k_{2o} = -k_{1o} \cot k_{1o}a \quad (11)$$

where $(k_{1o}a)$ must be between $\pi/2$ and π, $3\pi/2$ and 2π, etc.

Solution of the Conditional Equation and Mode Designation

Since the propagation constant must be the same in all regions, the following equations must be satisfied:

$$k_{1e}^2 - \omega^2\mu_0\epsilon_1 = -k_{2e}^2 - \omega^2\mu_0\epsilon_2 \quad (12)$$

$$k_{1o}^2 - \omega^2\mu_0\epsilon_1 = -k_{2o}^2 - \omega^2\mu_0\epsilon_2. \quad (13)$$

By substituting (10) into (12) (eliminating k_{2e}), and substituting (11) into (13) (eliminating k_{2o}), the following equations result.

$$\pi^2\left(\frac{2a}{\lambda_0}\right)^2(K_1 - K_2) = \left[\frac{k_{1e}a}{\cos k_{1e}a}\right]^2, \text{ even modes} \quad (14)$$

$$\pi^2\left(\frac{2a}{\lambda_0}\right)^2(K_1 - K_2) = \left[\frac{k_{1o}a}{\sin k_{1o}a}\right]^2, \text{ odd modes} \quad (15)$$

where $K_1 = \epsilon_1/\epsilon_o$, $K_2 = \epsilon_2/\epsilon_o$, λ_o = free-space wavelength. Since (14) and (15) are transcendental, graphical techniques have been used to obtain their roots. If the quantities

$$y = \left[\frac{k_{1e}a}{\cos k_{1e}a}\right]^2 \quad \text{and} \quad y = \left[\frac{k_{1o}a}{\sin k_{1o}a}\right]^2$$

are plotted as functions of $(k_{1e}a)$ and $(k_{1o}a)$ over their respective restricted intervals, the curves of Fig. 2 will result. Both sets of curves can be plotted on the same graph since their intervals of applicability are contiguous and interlaced, but do not overlap. Each curve

corresponds to a different TE mode. Values of $(2a/\lambda_o)$ and (K_1-K_2) can be selected and a horizontal line corresponding to the equation

$$y = \pi^2\left(\frac{2a}{\lambda_0}\right)^2 (K_1 - K_2)$$

can be drawn across the family of curves of Fig. 2. The values of $(k_{1e}a)$ and $(k_{1o}a)$ at the intersections of the horizontal line and the curves are the roots of (14) and (15).

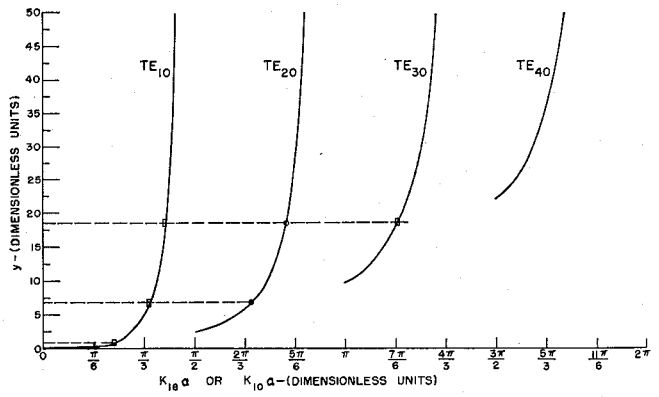

Fig. 2—Graphical technique for obtaining the roots of the conditional equation for the even and odd order TE modes.

It should be noted from Fig. 2 that the lowest order even mode $(o<k_{1e}a<\pi/2)$ can exist down to zero frequency. It is the dominant mode of this structure and will be designated the TE_{1o} mode. Successively higher modes will be designated TE_{2o}, TE_{3o}, etc. The mth mode is designated TE_{mo}. The even modes correspond to m being an odd integer, and vice versa. The zero shows that there is no variation of the fields in the y direction. Eqs. (14) and (15) show that in order for the TE_{mo} mode to propagate, the following inequality must be satisfied.

$$\frac{2a}{\lambda_o} > \frac{m-1}{2\sqrt{\Delta K}}, \qquad \Delta K = K_1 - K_2. \tag{16}$$

The procedure for obtaining the roots of (14) and (15), as shown in Fig. 2, was repeated for many values of $(2a/\lambda_o)$ and ΔK. The results for the dominant mode are shown in Fig. 3. The cutoff loci for various higher order TE modes are shown on this and many succeeding families of curves. Using the results of Fig. 3 and (10), values of $(k_{2e}a)$, the transverse distribution parameter for the outer regions, can be calculated as a function of $(2a/\lambda_o)$ and ΔK. The results of this calculation for the dominant mode are presented in Fig. 4.

The values of $(k_{1e}a)$ and $(k_{2e}a)$ are sufficient to enable one to plot the transverse field distributions. Sample plots of the field configuration, as well as graphs of the field magnitudes for the dominant mode (TE_{1o}) and the

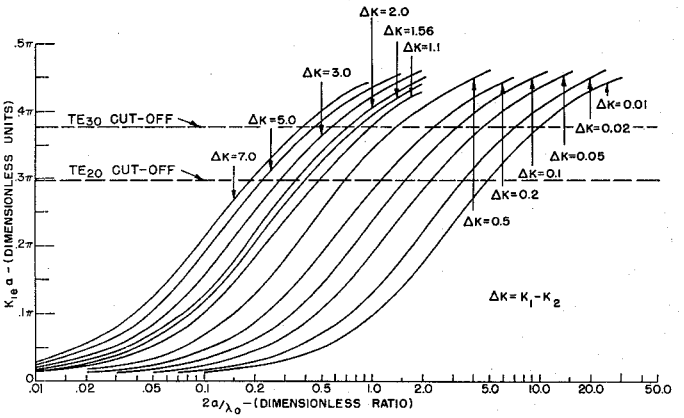

Fig. 3—Curves of the inner transverse distribution parameter $(k_{1e}a)$ of the dominant mode as a function of the normalized slab width $(2a/\lambda_o)$, and the difference of the dielectric constants (ΔK).

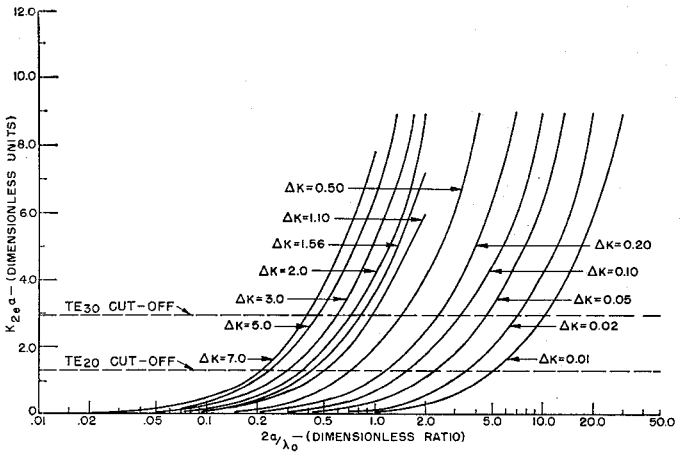

Fig. 4—Curves of the outer transverse distribution parameter $(k_{2e}a)$ of the dominant mode as a function of the normalized slab width $(2a/\lambda_o)$, and the difference of the dielectric constants (ΔK).

lowest order odd mode (TE_{2o}), are shown in Fig. 5 and Fig. 6. The amount of sinusoidal or cosinusoidal variation in Region 1 is determined by $(k_{1e}a)$, and the rate of exponential decay in Regions 2 and 3 is determined by k_{2e}, which is found from $(k_{2e}a)$.

It should be noted from (2) through (7) and Fig. 5 and Fig. 6, that none of the field components is a function of y. Guide wavelength, cutoff wavelength, and field extent of the TE modes are, therefore, independent of the distance b between the two conducting planes. This distance can be varied to suppress the hybrid modes, which are a function of y, and yet not cause cutoff of the TE modes. The cutoff criterion for the hybrid modes has been derived by Moore and Beam.[3] Their formula for determining the critical distance between the conducting planes, b_c, which suppresses all hybrid modes, is re-expressed below.

$$\frac{b_c}{\lambda_o} = \frac{1}{2}\sqrt{\frac{1+\tan^2 k_{1e}a}{1+K_1\tan^2 k_{1e}a}}. \tag{17}$$

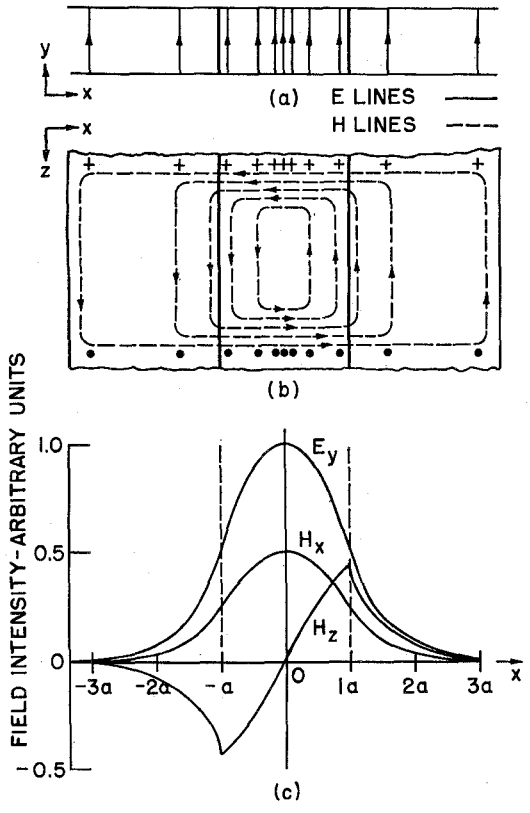

Fig. 5—(a) Cross-sectional view, and (b) top view of the field configuration of the dominant mode (TE_{1o}); (c) magnitude of the field components of this mode.

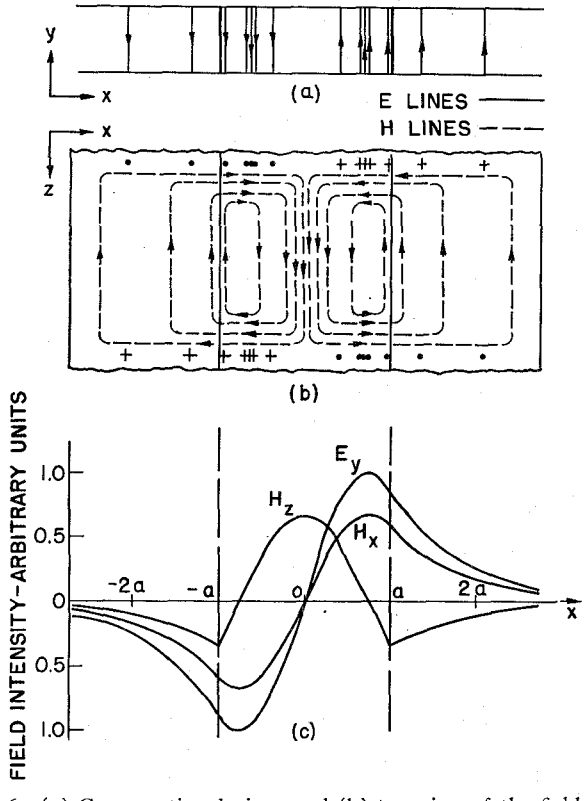

Fig. 6—(a) Cross-sectional view, and (b) top view of the field configuration of the lowest order antisymmetric mode (TE_{2o}); (c) magnitude of the field components of this mode.

This relationship is presented graphically in Fig. 7. Since TEM and TM modes cannot propagate on this line, only TE modes can exist if $b<b_c$. If, in addition, the following inequality is satisfied, single mode (TE_{1o}) operation is assured.

$$\frac{2a}{\lambda_o} < \frac{1}{2\sqrt{\Delta K}}. \tag{18}$$

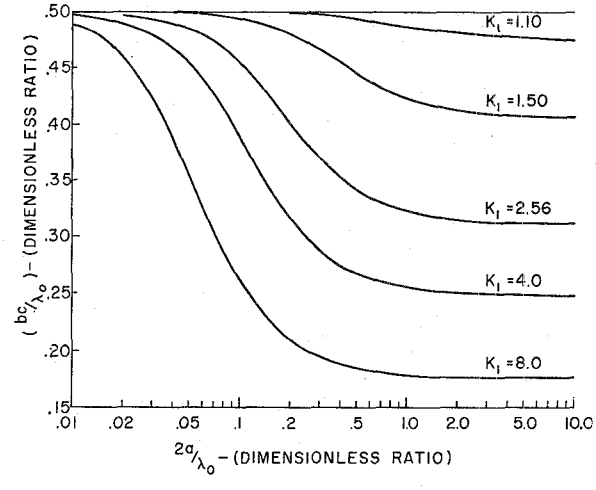

Fig. 7—Cutoff condition for the hybrid modes as a function of the normalized slab width ($2a/\lambda_o$) and dielectric constant (K_1).

If a conducting wall is placed at the $x=o$ plane, all of the even TE modes will be suppressed, but the odd modes will be unaffected. The dominant mode of the resulting trough line (half of the original line) will be the TE_{2o} mode.

The ratio of the cutoff wavelengths of the TE_{2o} and the TE_{4o} mode is 3:1. This modified structure, therefore, also has an inherent bandwidth advantage over conventional rectangular waveguide. Although it does not have the bandwidth capability of the TE_{1o} mode on the original line, it has the advantages of being a smaller guide and being closed on three sides. The trough line geometry is appropriate for the design of ferrite devices employing transverse magnetization.

Guide Wavelength

Making use of (8) and the fact that $\lambda_g = 2\pi/\beta$, it is easily shown that

$$\frac{\lambda_g}{\lambda_o} = \frac{\pi\left(\frac{2a}{\lambda_0}\right)}{\sqrt{\pi^2\left(\frac{2a}{\lambda_0}\right)^2 K_1 - (k_{1e}a)^2}}, \quad \text{even modes.} \tag{19}$$

The corresponding expression for the odd modes is the same as (19) except that $(k_{1o}a)$ replaces $(k_{1e}a)$. For the case where the outer regions are air or vacuum ($K_2=1$), λ_g/λ_o has been calculated for the TE_{1o} and TE_{2o} modes.

The results of these calculations are shown in Fig. 8 and Fig. 9. For small values of $(2a/\lambda_o)$, (λ_g/λ_o) approaches unity; and for large values of $(2a/\lambda_o)$, (λ_g/λ_o) approaches $1/\sqrt{K_1}$. This result is in agreement with the transverse field distribution picture of this mode, since small values of $(2a/\lambda_o)$ correspond to most of the energy being propagated in regions 2 and 3, and large values of $(2a/\lambda_o)$ correspond to most of the energy confined in the dielectric slab. The cutoff loci for higher order TE modes are shown as dashed curves superimposed on the λ_g/λ_o curves.

Power Handling Capabilities

Since $E_x = H_y = 0$, and the product $E_y H_x$ is an even function of x, the axial power flow is

$$P_z = -\,\text{Real}\int_{y=o}^{y=b}\left[\int_{x=o}^{a} E_{y1}H_{x1}^{*}\,dx + \int_{x=a}^{\infty} E_{y3}H_{x3}^{*}\,dx\right]dy. \quad (20)$$

If the proper expressions from (2) through (7) are inserted in (20), and the indicated integration is performed, the following formulas for the power flow of the even and odd modes result:

$$P_{ze} = |A_e|^2 \pi ba \sqrt{\frac{\mu_0}{\epsilon_0}}\left(\frac{2a}{\lambda_0}\right)\frac{\sqrt{\pi^2 K_1\left(\frac{2a}{\lambda_0}\right)^2 - (k_{1e}a)^2}}{2(k_{1e}a)^2}\cdot\left[1+\frac{\cot k_{1e}a}{k_{1e}a}\right] \quad (21)$$

$$P_{zo} = |A_o|^2 \pi ba \sqrt{\frac{\mu_0}{\epsilon_0}}\left(\frac{2a}{\lambda_0}\right)\frac{\sqrt{\pi^2 K_1\left(\frac{2a}{\lambda_0}\right)^2 - (k_{1o}a)^2}}{2(k_{1o}a)^2}\cdot\left[1-\frac{\tan k_{1o}a}{k_{1o}a}\right]. \quad (22)$$

For the dominant mode, the maximum electric field is located at $x=0$. As a safety factor, the breakdown power level P_{bd} will be calculated assuming that the maximum electric field E_{bd}, which can exist at $x=0$, is the breakdown field of air (despite the fact that a dielectric material occupies this central region). E_{bd} will be taken as 15,000 volts per centimeter (a safety factor of approximately 2) to conform to standard waveguide calculations. From (2c) it is seen that at $x=o$

$$|A_e| = \frac{k_{1e}}{\omega\mu_0}|E_{bd}|. \quad (23)$$

If (23) is substituted into (21), the following equation is obtained for the breakdown power level of the dominant mode.

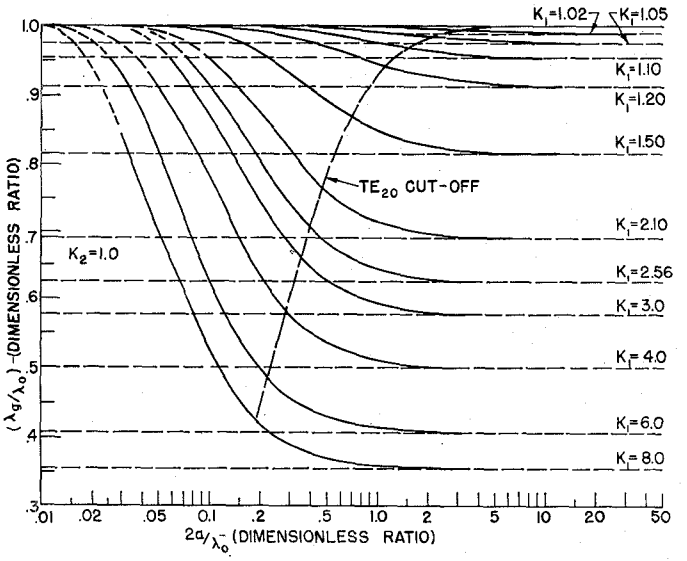

Fig. 8—Curves of the normalized waveguide wavelength (λ_g/λ_o) of the dominant mode, for the case where the outer regions are air or vacuum, as a function of the normalized slab width $(2a/\lambda_o)$ and dielectric constant (K_1).

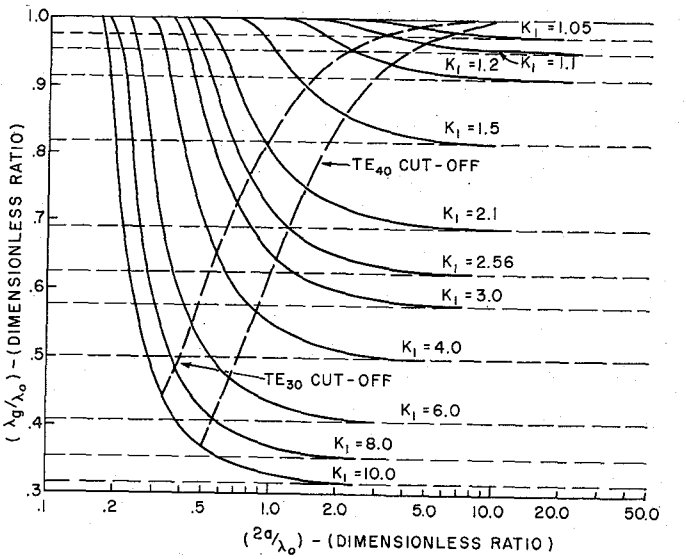

Fig. 9—Curves of the normalized waveguide wavelength (λ_g/λ_o) of the TE_{2o} mode, for the case where the outer regions are air or vacuum, as a function of the normalized slab width $(2a/\lambda_o)$ and dielectric constant (K_1).

$$\frac{P_{bd}}{ab} = \frac{9.51\cdot 10^8}{(2a/\lambda_o)}\left[1+\frac{\cot k_{1e}a}{k_{1e}a}\right]\cdot\sqrt{\pi^2 K_1\left(\frac{2a}{\lambda_0}\right)^2 - (k_{1e}a)^2}. \quad (24)$$

For the case where $K_2=1$, this function has been calculated for many values of $(2a/\lambda_o)$ and K_1. The resulting family of curves is shown in Fig. 10. These curves show that for very small values of $(2a/\lambda_o)$, which corresponds to a very loosely bound wave, P_{bd} becomes very large. Any practical transmission line will have to be of finite

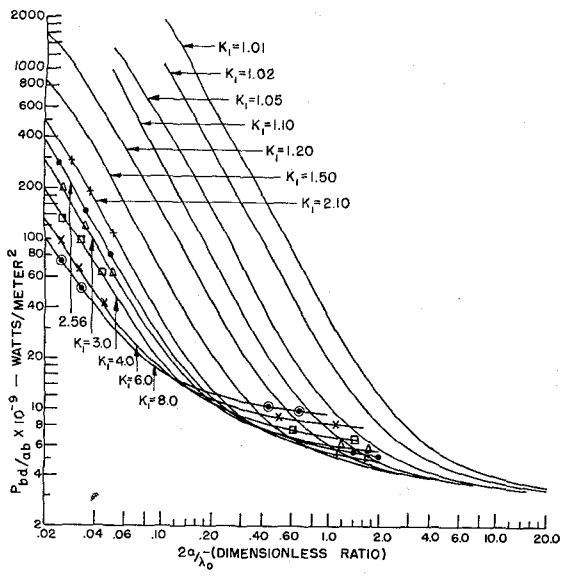

Fig. 10—Curves of the power handling capability ($P_{bd}ab$) as a function of the normalized slab width ($2a/\lambda_o$) and dielectric constant (K_1). These curves are for the dominant mode and the case where the outer regions are air or vacuum.

extent in the x-direction, and hence there is a practical lower bound on ($2a/\lambda_o$) and an upper bound on the power handling capability. The improved power handling capabilities of this line are a result of its larger size and resultant reduced power density. The advantage is that single mode operation can be assured even with the large waveguide. The curves of Fig. 10 should provide an accurate measure of the power handling capacity if the width of the guide (in the x-direction) is sufficiently large so that nearly all of the power is propagated in the region between the two conducting planes.

Transmission Losses

Thus far, it has been assumed that the two parallel conducting planes had infinite conductivity and that the dielectric material had zero conductivity. This ideal line, of course, will have no losses. Practical transmission line conductors will have large but finite conductivity and the dielectric will have small but finite conductivity. Approximate attenuation formulas will be derived for these low loss materials. Since these losses are assumed to be small, separate equations can be derived for the wall loss and the dielectric loss.

The wall loss per unit length in the z-direction P_w is given by:

$$P_w = 2\cdot\frac{1}{2} R_s \int_{-\infty}^{\infty} |H_t|^2 dx, \tag{25}$$

where $R_s = \sqrt{\omega\mu_o/2\sigma_w}$ = surface resistance of the metal walls,

$|H_t| = (|H_x|^2 + |H_z|^2)^{1/2}$

= magnitude of the magnetic field at the walls

σ_w = conductivity of the metal walls.

The extra factor of two in (25) accounts for the two conducting walls. The attenuation per unit length due to the wall loss is

$$\alpha_w = \frac{P_w}{2P_z}\cdot \tag{26}$$

The proper expressions for the magnetic field should be substituted into (25), and the integration performed. If the resulting expression and either (21) or (22) are then substituted in (26), the following equations for the attenuation due to the wall loss for the even and odd TE modes result.

$$\alpha_{we} b\sqrt{\lambda_0} = \frac{.0291}{\sqrt{\sigma_w}} \cdot \frac{\left[\pi^2 K_1 \left(\frac{2a}{\lambda_0}\right)^2 - \frac{(k_{1e}a)^2 \cot k_{1e}a}{k_{1e}a + \cot k_{1e}a}\right]}{\left(\frac{2a}{\lambda_0}\right)\sqrt{\pi^2 K_1 \left(\frac{2a}{\lambda_0}\right)^2 - (k_{1e}a)^2}} \tag{27}$$

$$\alpha_{wo} b\sqrt{\lambda_o} = \frac{.0291}{\sqrt{\sigma_w}} \cdot \frac{\left[\pi^2 K_1 \left(\frac{2a}{\lambda_0}\right)^2 (k_{1o}a - \tan k_{1o}a) + (k_{1o}a)^2 \tan k_{1o}a\right]}{\left(\frac{2a}{\lambda_0}\right)(k_{1o}a - \tan k_{1o}a)\sqrt{\pi^2 K_1 \left(\frac{2a}{\lambda_0}\right)^2 - (k_{1o}a)^2}}. \tag{28}$$

For the case of the dominant mode, and for $K_2 = 1$, (27) has been plotted in Fig. 11 for a range of ($2a/\lambda_o$) and many values of K_1. The conductivity of copper ($\sigma_w = 5.80\times 10^7$ mhos per meter) was used in this computation. The curves of Fig. 11 can be used for other wall materials if the values of attenuation obtained from them are multiplied by the square root of the relative resistance of the substituted material.

The equation for the dielectric attenuation is derived for the case where Regions 2 and 3 are air or vacuum, and hence the dielectric loss all occurs in Region 1. The dielectric loss per unit length in the z-direction P_d is given by

$$P_d = \frac{\sigma_d}{2}\int_{y=0}^{b}\int_{x=-a}^{+a} |E_{y1}|^2 dx dy, \tag{29}$$

where $\sigma_d = \omega\epsilon_o K_1 \phi_d$ = conductivity of the dielectric material,

ϕ_d = loss tangent of the dielectric material.

The attenuation per unit length due to the dielectric loss is

$$\alpha_d = \frac{P_d}{2P_z}\cdot \tag{30}$$

The proper expressions for the electric field, (2c) or (5c), should be inserted in (29) and the integral evaluated to

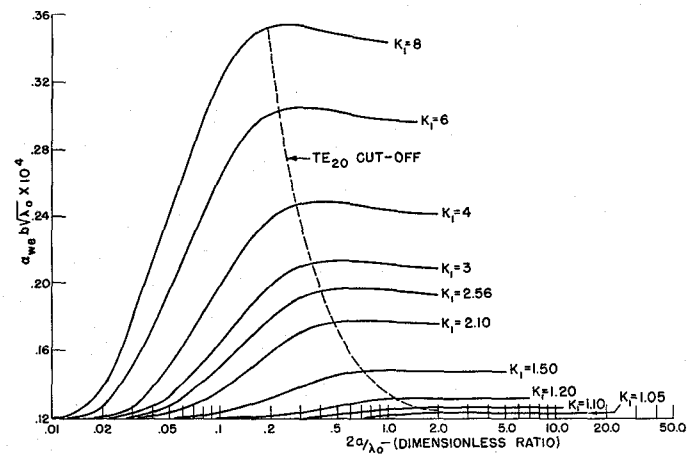

Fig. 11—Attenuation (in nepers per meter) due to the loss in the walls as a function of the normalized slab width ($2a/\lambda_0$) and dielectric constant (K_1). These curves are for the dominant mode and the case where the outer regions are air or vacuum and the wall material is copper ($\sigma = 5.80 \times 10^7$ mhos per meter).

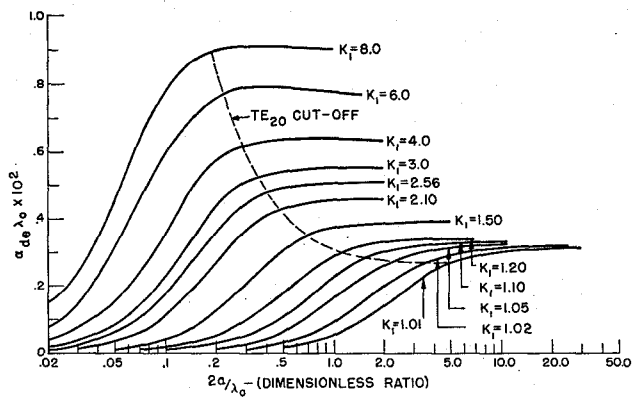

Fig. 12—Attenuation (in nepers per meter) due to the dielectric loss as a function of the normalized slab width ($2a/\lambda_0$) and dielectric constant (K_1). These curves are for the dominant mode and the case where the outer regions are air or vacuum. The loss tangent (ϕ_d) equals 0.001.

obtain equations for the dielectric power loss of the even and odd TE modes. The resulting expressions and either (21) or (22) are substituted into (30) to obtain the following formulas for the attenuation due to the dielectric loss.

$$\alpha_{de}\lambda_0 = \frac{\pi^2 K_1 \phi_d \left(\frac{2a}{\lambda_0}\right)}{\sqrt{\pi^2 K_1 \left(\frac{2a}{\lambda_0}\right)^2 - (k_{1e}a)^2}} \cdot \left[\frac{k_{1e}a + \sin k_{1e}a \cos k_{1e}a}{k_{1e}a + \cot k_{1e}a}\right] \tag{31}$$

$$\alpha_{do}\lambda_o = \frac{\pi^2 K_1 \phi_d \left(\frac{2a}{\lambda_0}\right)}{\sqrt{\pi^2 K_1 \left(\frac{2a}{\lambda_0}\right)^2 - (k_{1o}a)^2}} \cdot \left[\frac{k_{1o}a - \sin k_{1o}a \cos k_{1o}a}{k_{1o}a - \tan k_{1o}a}\right]. \tag{32}$$

Fig. 12 is a plot of $\alpha_{de}\lambda_o$ as a function of ($2a/\lambda_o$) and many values of K_1 for the dominant mode. These calculated results were plotted for a value of dielectric loss tangent $\phi_d = 0.001$. These curves can be used for other values of ϕ_d if the values of α_d obtained are divided by 0.001 and multiplied by the loss tangent of the dielectric used.

Discussion

The parallel plane waveguide partially filled with a dielectric can support a class of TE modes, whose field structure is similar to the TE_{mo} modes of rectangular waveguide. These TE modes display either even or odd symmetry about the geometrical plane of symmetry ($x = o$). It is not possible to support TEM or TM waves on this structure. It has been previously shown that hybrid modes can also propagate on this line.[1–3] A sufficiently small, yet convenient, value for the distance between the conducting planes can be found which will suppress the hybrid modes and not affect the TE modes.

The dominant mode of this line (TE_{1o}) has no cutoff frequency, and hence it is inherently capable of very wide bandwidth operation. For a loosely bound wave, the losses are comparable to those of conventional rectangular waveguide, and the power handling capacity is an order of magnitude greater. In order to obtain the advantages of a loosely bound wave on this line, the structure must be substantially larger than rectangular waveguide. This line may, therefore, offer its greatest utility at millimeter wavelengths, where its size is still convenient. The availability of low loss, low dielectric constant materials allows the use of a reasonably wide dielectric center strip. The dielectric strip will, therefore, be mechanically self-supporting, while retaining the advantages of a loosely bound wave structure even at millimeter wavelengths. In the case of the dielectric loaded trough guide propagating the TE_{2o} mode, thin layers of higher dielectric constant materials can be supported alongside the vertical conducting wall.

Acknowledgment

The author would like to thank Dr. M. E. Brodwin and J. C. Wiltse for their helpful discussions and criticisms. Acknowledgment is due Miss M. D. Velten and Mrs. B. H. Medcalf for the numerical calculations and curve plotting.